Study the Influence of Gas Pressure on the Tensile Behavior of TIG Stainless Steel Sheets

Samir Ali Amin Al-Rabii

Department of Mechanical Engineering, University of Technology, Baghdad-Iraq

alrabiee2002@yahoo.com

Lamyaa Mehdi Assad

Department of Mechanical Engineering, University of Technology, Baghdad-Iraq

lmy_asr@yahoo.com

Ali Hussein Alwan

Department of Mechanical Engineering, University of Technology, Baghdad-Iraq

eng.ali83@yahoo.com

Submission date:- 4/7/2018	Acceptance date:- 12/8/2018	Publication date:- 27/8/2019

Abstract

This research work represents the study of the effect of using different gas pressures of argon on the tensile behavior of tungsten inert gas (TIG) welded stainless steel sheets type (304). Different ranges of gas pressures (13-15 Kgf/cm^2)and welding currents (80-100 Apm) were used to determine their influenceon the tensile mechanical properties (0.2% yield stress, ultimate tensile stress and elongation) of butt welded joints.Design of experiment (DOE) 'version 10' was used to establish the design matrix of experiments. Response surface methodology (RSM) technique was employed to obtain mathematical models for the three properties, which were analyzed by the analysis of variance (ANOVA) to verify statistically the adequacy of the resulted models. The resultant quadratic models with a confidence level of 95% revealed thatthe increase in both gas pressure and currentindividually results in a higher increase in the yield stress and elongation,and both were proportionated inversely,while their combined effect gave the lowest values.The gas pressure had a greater impact on the ultimate tensile stress than current. After numerical optimization, the maximum values of the mechanical properties were obtained with a maximum desirability value at the optimum values of gas pressure and current. Finally, confirmation tests were conducted at the optimum values of gas pressure and current to verify the validation of the maximum values of properties, and the error wasfound less than (4%) between the experimental and predicted results.

Keywords: TIG welding, Gas Pressure, Mechanical Properties, Design of Experiment, Response Surface Methodology, Numerical Optimization.

1.Introduction:

Presently, outputs and features of goods represent a significant part in the industrial market. The weld features are related to the best choice of main welding factors, such as welding current, voltage, filler material and welding speed. Trying to develop the mechanical characteristic via initial annealing could be important when the welding factors like groove model and filler angle are considered. In this research an attempt was dove to figure out the influence of TIG welding factors, including the gas flow rate for stainless steel (304) sheets by using argon gas. There are many variables that can be considered when choosing the welding methods. In numerous manufacturing fields, the most common gas shielding arc-welding process used is tungsten inert gas (TIG) welding. Even though there are other arc- welding processes but when compared with the (TIG) welding processes, they have limited features. However, many properties of TIG welding are needed to progress, such as spatter decrease and weld quality of the bead. Conservation of atmospheric pollution is preferable using a shielding gas to the TIG welding operation. [1]. In TIG welding processes, power source, a shielding gas, and TIG holder are needed. The main source is feeding the power that is down the TIG holder and then is transmitted to tungsten electrode that is suited with the holder. After that, an electric arc between the tungsten electrode and the work sample will be created Two kinds of welding that most commonly used for joining stainless steels are called manual and automatic gas tungsten arc welding (GTAW) processes, mostly in thickness up to around(5mm) [2].

2.Literature Review

In this part, a general review of TIG welding operation, apparatuses, energy resource, pattern of electrode, covering gases, kinds of current and gas flowing is illustrated.

Singh, et .al. [3]. Stated that raising in temperature on work sample face achieved through rising the welding current that caused as rising the face width and rear width of weld joint linearly. They also found out that the dimensions of weld joint reduce linearly with increase of welding velocity, but rising depth permeation. The mechanical features of weld joint influenced highly with change of welding factors, while the dimensions of weld joint changed up and down with rising of gas flux. Patel and Patel in (2014) [4] discussed the influence of TIG welding factors, like welding current, gas flux and welding velocity which are impact on reacting product factors like solidity of welding tensile intensity of welding, through relating optimization philosophy. Mishral, et al. [5]. Investigated stainless steel of degrees (202, 304, 310 and 316) jointed with moderate steel through tungsten lazy gas (MIG) welding operations. Also, they predicted the proportion reduction of the welded joints and found out tensile intensity of different mineral links. The output for various joints achieved by TIG and MIG welding operation were compared, the out hors pointed out that TIG welded various mineral joints own best physical features than MIG welded joints. Rao, and Deivanathan [6]. Studied the welding variables, such as current, filler substance, and welding velocity and investigated the mechanism characteristic and construction of 310 austenitic stainless steel through applying a stainless steel filler substance for various levels. Also, they have achieved maximum tensile stress with a current 120A and 309L filler bar.Prabaharan et al. [7]. Experimentally studied the optimization a welding parameters in the gas tungsten Arc welding of Inconel 825 alloyusing a factorial design method for parametric optimization. The investigated welding parameters selected were welding voltage, welding current, gas flow rate, nozzle to plate distance and torch angle and weld deposit area was optimized for the above parameters. A mathematical model is developed by Factorial design approach to find out the relationship between the various processes the most important requirement for all welding is weld deposition area that determines the characteristics of the weld. Experiment results suggested that the increase in the welding current, gas flow rate, and torch angle increases weld deposit area and increase in voltage and nozzle to plate distance decreases the weld deposit area. Ravinder and Jarial [8]. Studied the influence of welding current, arc voltage, and gas flow rate on strength of SS-202 and mild steel material through welding. The study found that the control factors had varying effects on the tensile strength, arc voltagehaving the highest effect. Taguchi method has been very successful in designing high quality products and processes of many different fields. Taguchi design of experiment technique can be very efficiently used in the optimization of welding parameters in manufacturing operations. Gurdev and Bansal [9] studied the weld quality that influenced by weld bead geometry through a joining process. Tests the performed welding procedure for figuring out the bead geometry variables of welded joints. This research also involved with the design and optimization of bead geometry variable for tungsten inert gas (TIG) welding operations and then bead geometry strength. Taguchi and ANOVA style were applied to manage the best results. The study found that the control factors had varying effects on the Tensile strength, welding voltage having the highest effects Optimum parameter setting for weld strength is obtained at current of 160 amps, 35 volt, and 10-litre/min-gas flow. Ravichandran, et al.in [10] were studied for duplex stainless steel (2205) using SN ratio and ANOVA analysis. Welding current, gas flow rate and welding speed were considered as the welding parameters and impact strength and hardness were taken as responses. From the SN ratio analysis, it was concluded that high impact strength can be obtained when the welding current was 150 A, gas flow rate was 14 L/min and the welding speed was 210 mm/min. Also, the high hardness of the joints could be obtained when the welding current was 190 A, gas flow rate was 12L/min and the welding speed was 175 mm/min. SEM images for base metal and the welded zone of welded joints were reported. The dendrite structure was observed in the weldment region. ANOVA analysis indicated that the gas flow rate was the most significant parameter for both impact strength and hardness of the joints. N Kumar Rahul and Vijay Mittal in [11] they studied the mechanical properties of the joint of austenitic stainless steel (AISI 316) and mild steel welded by TIG welding. In this paper with the use of Taguchi method of optimization we have tried to optimized the various process parameter such as current, voltage and gas flow ratio (GFR) which has influence on tensile strength and hardness of the joint. In this experiment Taguchi design is used for the optimization of welding parameters for the joint of stainless steel (AISI 316) and mild steel. Optimized parameters for the tensile strength are 100, 26, and 10 with different values of arc current, arc voltage and gas Flow rate. Optimized parameters for the Hardness are 100,18 and 314 with different values of arc current, arc voltage and gas flow rate.

3. Experimental Work

3.1. Material selection and preparation of specimens

The sheet of stainless steel 304 alloy was used in this work which obtained from a localmarket with a thickness of (2 mm). The chemical composition of this alloy is shown in table (1) according to the standard material ASTM (A240)[12]. These sheets material were cut to the required dimensions (210 mm x110 mm) by an electrical cutting machine to prepare the welding specimens, and the their edge were ground to ensure that there is no gap between the two sheets, as shown in Figure (1).

Table (1):Chemical composition of used stainless steel 304 alloy

Wt. %	C	Mn	P	S	Si	Cr	Ni	Mo	N
Stainless steel 304 [12]	0.08	2	0.045	0.03	0.75	18	8	-	0.1

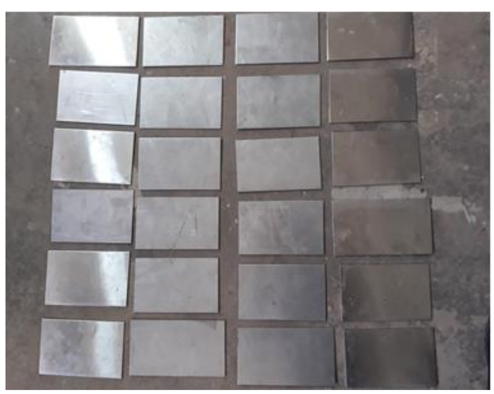

Figure (1):Preparation of the weld specimens

3.2 Weldingprocess procedure

The TIG welding process was performed manually by a skillful welder in the University of Technology / Workshop Center. Before welding the twosheetswere fixed firmly on the welding table and clamped tightly into their place, as shown in figure (2). In this work, the power TIG 160 welding machine was used to weld the sheets, as shown in figure (3). The main technical data used of the welding machineand welding toolsare listed in table (2). The argon gas was used as the inert gas through the welding process, and the gas flow can be adjusted manually by argon gas regulator, as shown in figure (4).The 304 filler is suitable with the base material of 304 stainless steel.To obtain the desired high quality of TIG welded joints with high mechanical properties, i.e., high TIGwelding efficiency, the main chosen welding parameters are (current and gas pressure) to determine the effect of each parameter on the mechanical properties.

Table (2):The main technical data of welding machine

Power factor	0.69
Open-circuit voltage	65-80V
Open-circuit power	30W
Tungsten electrode diameter	1.6 mm
Filler rod diameter	1.6 mm

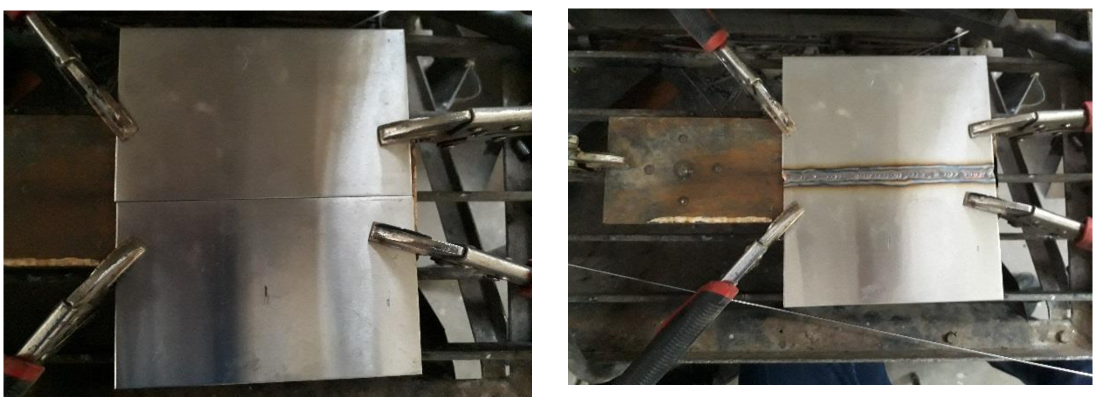

(a) Before welding **(b) After welding**

Figure (2):Workpiecebeforeandafter welding

Figure (3): Welding Machine

Figure (4): Argon Gas Regulator

3.3 Experimental design matrix

In the present research, the DESIGN EXPERT 8 program with response surface methodology (RSM) technique was used to build the input matrix. Input parameters used in the experimentation processes were selected depending on the practical experience previous research works. These factors areshown in Table (3) with two levels. The used experimental design was performed by (RSM) using a central composite rotatable design for two input factors, and three outputs(responses), with fivecenter points and four axial points. Thirteen runs were carried out according to the experimental design matrix. Each parameter was used at two coded levels (−1and +1), where each level conformed to areal value tantamount to the coded value. Thus, the input parameters studied are welding gas flow pressure and current. The input parameters in terms of actual factors are given in Table (4), which represents the used experimental design matrix.

Table (3): Usedlevels of Input Parameters with Respective Coding

Factor	Unit	Low Level (-1)	High Level (+1)
Gas Flow Pressure	Kgf/cm^2	13	15
Current	Amp.	80	100

Table (4) Experimental design matrix for both actual input factors and responses

Standard No.	Run No.	Gas Pressure (Kgf/cm^2)	Current Amp.	Yield Stress(MPa)	Ultimate Tensile Stress (MPa)	Elongation (%)
1	2	13	80	240	535	28
2	8	13	100	298	527	44
3	3	15	80	335	715	44
4	1	15	100	270	703	20
5	4	14	70	272	606	38
6	7	14	110	272	570	27
7	9	12	90	268	313	40
8	6	16	90	320	660	31
9	10	14	90	285	694	31
10	13	14	90	285	695	35
11	12	14	90	298	715	32
12	5	14	90	300	710	34
13	11	14	90	290	711	35

3.4 Mechanical properties tests

In the present work, the tensile tests were carried out in University of Technology/Department of Mechanical Engineering. These tests were done at room temperature using Tinius Olsenuniversal testing machine which has a maximumcapacity of (5KN), as shown in figure (5). The tensile specimens were made by a CNC milling machine, and the specification of the tensile test was restricted according to the American Society for Testing and Materials specifications (ASTM). The tensile specimen's geometry and dimensions for standard (ASEM E8-M) [13] are depicted in figure (6). The average of three specimens for each welding case wastaken in a perpendicular direction to the welded line, and tested at a constant crosshead speed of (1mm/min) to determine the tensile properties of each welding joint,figure (7). The

experimental obtained values of tensile strength, yield stress, and elongation are also given in Table (4).

Figure (5): Tinius Olsen universal testing machine

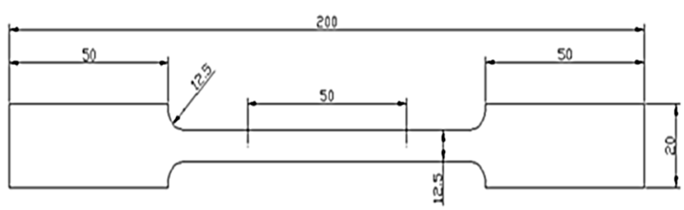

Figure (6): Rectangular cross section tensile test specimen according to ASTM E8-M.[13]
All dimensions are in millimeters

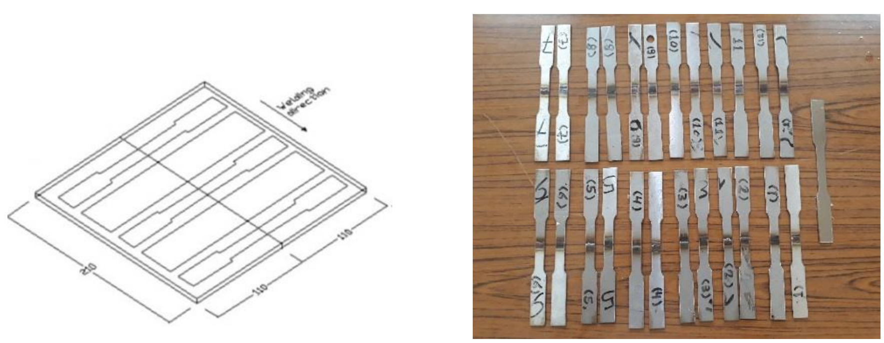

Figure (7):Tensile test specimens

4.Results and Discussion

4.1 The 0.2% yield stressmodel

The average responses obtained for yield stress,elongation and tensile strength were used in calculating the models of the response surface per response using the least-squares method.

For 0.2% yield stressprediction, a reduced quadratic model in coded terms was analyzed with backwards elimination of insignificant coefficients. Table 5 depicts the statistical analysis of variance (ANOVA) produced by the software for the remaining terms. The model is significant at 95% confidence.It is noticed that the current (A), gas pressure (B), and the interaction of these factors (AB) are significant terms. The lack of fit test indicates a good model. This model illustrates that only the three terms (A, B, and AB) have the highest impact on the 0.2% yield stress.

Table 5: ANOVA for response surface quadratic model for 0.2% yield stress

Source	Sum of Squares	df	Mean Square	F Value	P-value Prob> F
Model	6868.67	4	1717.17	52.63	<0.0001**significant**
A-Current	4381.07	1	4381.07	134.27	<0.0001
B-Gas Pressure	4164.64	1	4164.64	127.64	<0.0001
AB	3782.25	1	3782.25	115.92	<0.0001
A^2	645.58	1	645.58	19.79	0.0021
Residual	261.02	8	32.63		
Lack of Fit	59.82	4	14.96	0.30	0.8665 **not significant**
Pure Error	201.20	4	50.30		
Cor Total	7129.69	12			
Std. Dev.5.71			**R-Squared** 0.9634		
Mean 287.15			**Adj. R-Squared** 0.9451		
C.V. %1.99			**Pred. R-Squared**0.9251		
PRESS533.71			**Adeq. Precision**25.406		

The final equation of 0.2% yield stress in terms of the actual factors is:

Yield stress = - 4189.14815 + 52.15278 * Current + 291.00000 * Gas Pressure

- 3.07500 * Current * Gas Pressure – 0.050895 Current^2…. **(1)**

Looking at the normal probability plot (figure 8) for the 0.2% yield stress data, the residuals generally that falling on a straight line implying errors, are normally distributed. Also, according to figure 9 that depicts the residuals versus predicted responses for elongation data, it is noted that there are no obvious patterns or unusual structure, implying models are accurate.

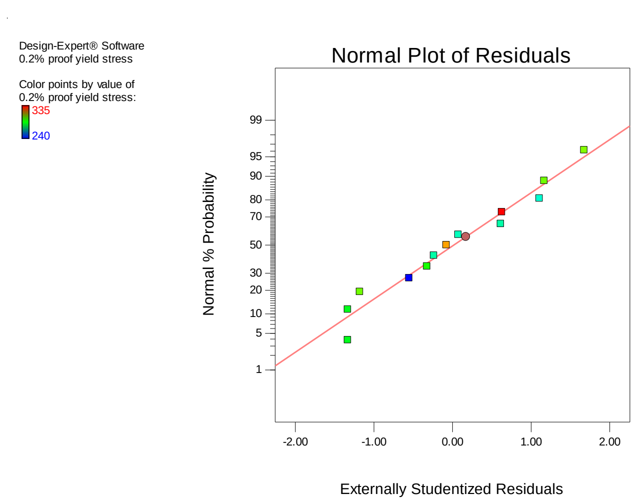

Figure (8): Normal distribution of yield stress data

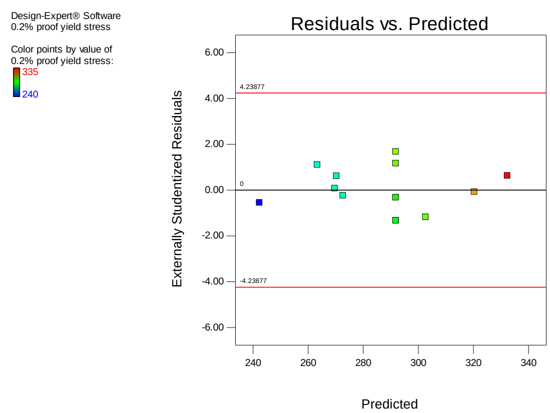

Figure (9): Residual versus predicted data

Figure 10 manifests the predicted actual 0.2% yield stress data versus the actual ones for comparison reason,andfigure 11 reveals the perturbation of 0.2% yield stress which shows the effect of both current and gas pressure on the yield stress over the range of the used levels; the gas pressure has a greater impact on the yield stress than current. Whereas, figure 12 displays that the interaction (combined influence) of both factors occurs after the center (at almost 95 Amp current).

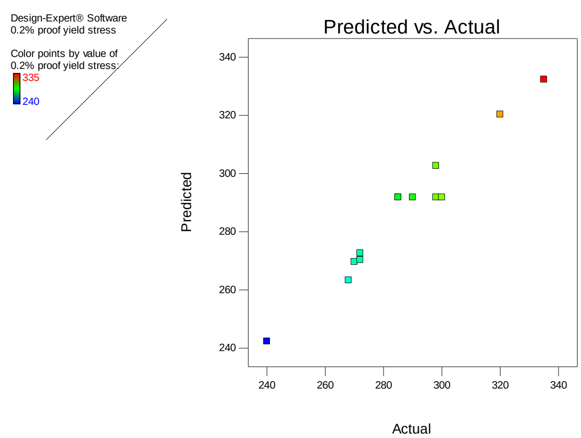

Figure (10): Predicted versus actual data

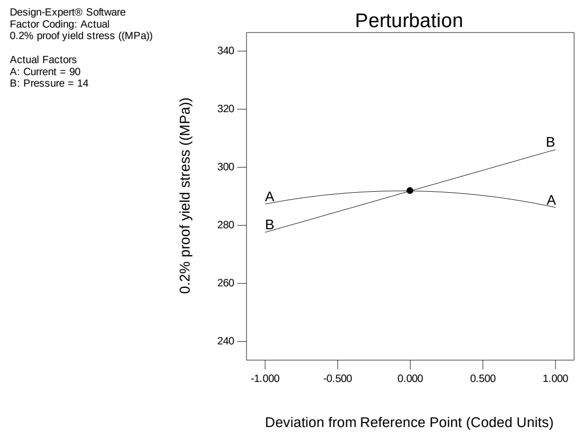

Figure (11): Perturbation of 0.2% yield stress

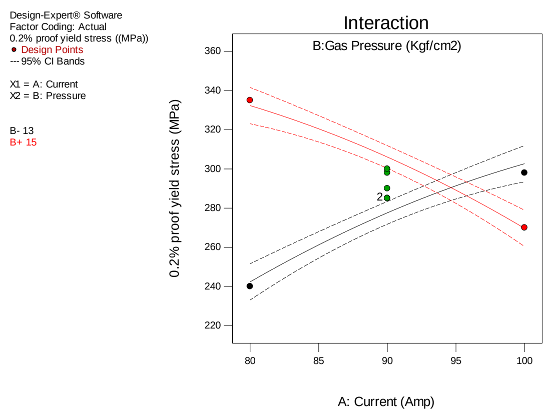

Figure (12): Interaction of the current with the gas pressure

Figure 13 reveals the 2D contour graph of 0.25 yield stress as a function of current and gas pressure.According to this figure, it can benoticed that the increase in both gas pressure and currentindividually leads to a higher increase in the elongation. The increase in the gas pressure at lower current (80 Amp)resulted inmore than (320 MPa) yield stress due to the more protection of the weld joint caused by the higher gas pressure, while the increase in the current (100 Amp) at lower gas pressure (13 Kgf/cm2) resulted in more than (300 MPa) yield stress due to the higher thermal effect caused by the higher heat input at higher current. This means that both gas pressure and current have a greater influence on the yield stress individually and they proportionate inversely. Regarding the interaction of gas pressure and current, this figure also shows that at almost (95 Amp and 14 Kgf/cm2), the combined influence of both factors gives a lower yield stress (about 290 MPa) than that caused by each one individually.

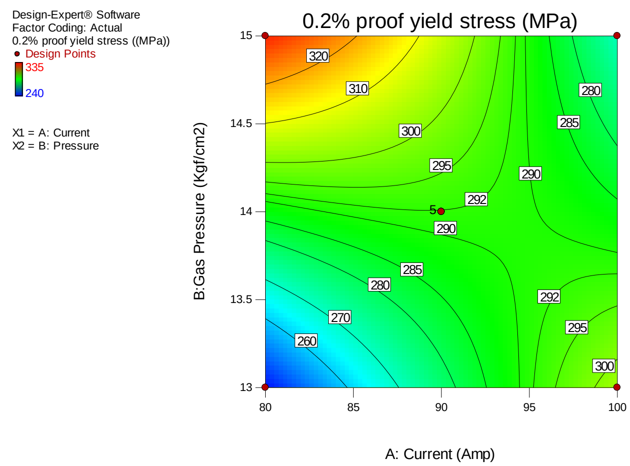

Figure (13): 2D contour graph of yield stress as a function of current and gas pressure

Figure (14) views the 3D graph (surface plot) of 0.2% yield stress as a function of gas pressure and current and confirms the observations mentioned above in the 2D graph. It can be noticed that the increase of both gas pressure and current caused an increase in the yield stress value at their higher level, while the increase of gas pressureisslightly higher, while at almost near their center level (design center point), their combined effect gave the lowest value of yield stress.

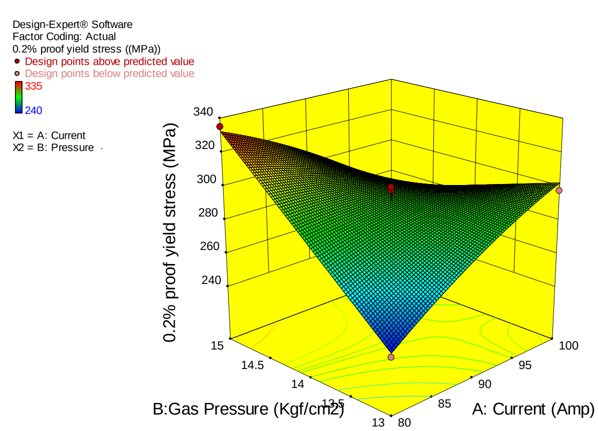

Figure (14): 3D surface plot of yield stress as a function of current and gas pressure

4.2 The ultimate tensile stress model

Similarly, for tensile stress results given in Table 4, a reduced quadratic model in coded terms was analyzed with backwards elimination of insignificant coefficients.

Table 7 reveals the statistical analysis of variance (ANOVA), and this model is significant at 95% confidence. In such model, the current (A), gas pressure (B) and their squared terms (A^2) and (B^2) are all significant. This model indicates that these four terms have the highest impact on the ultimatetensile stress. Also, there is no interaction between the current and gas pressure. The lack of fit test indicates a good model.

Table 6: ANOVA for response surface quadratic model for ultimate tensile stress

Source	Sum of Squares	df	Mean Square	F Value	P-value Prob >F
Model	1.657E+005	4	41428.66	743.69	<0.0001**significant**
A-Current	705.33	1	705.33	12.66	0.0074
B-Gas Pressure	91875.00	1	91875.00	1649.25	<0.0001
A^2	19630.01	1	19630.01	352.38	<0.0001
B^2	68420.18	1	68420.18	1228.21	< 0.0001
Residual	445.66	8	55.71		
Lack of Fit	63.66	4	15.91	0.17	0.9446 **not significant**
Pure Error	382.00	4	95.50		
Cor Total	1.662E+005	12			
Std. Dev.7.46			**R-Squared** 0.9973		
Mean 287.15			**Adj. R-Squared** 0.9960		
C.V. %1.19			**Pred. R-Squared**0.9935		
PRESS1074.38			**Adeq. Precision**87.459		

The final equation of ultimate tensile stress in terms of the actual factors is:

Ultimate tensile stress = -13532.43319 +51.91825 * Current +1617.54310 * Gas Pressure - 0.29269 * $Current^2$ – 54.64440 * Gas $Pressure^2$ … **(2)**

For checking statistically the adequacy of this model, the normal probability plot of residuals for tensile strength data showed that the residuals (errors) fall generally on a straight and they are normally distributed. Also, there are no obvious patterns or unusual structure, implying models are accurate.

Figure 15 shows the predicted versus actual tensile strength data for comparison purpose. And Figure 16 illustrates the perturbation of ultimate tensile stress which shows the effect of both current and gas pressure on the ultimate tensilestress over the range of the used levels; the gas pressure has a greater impact on the ultimate tensilestress than current.

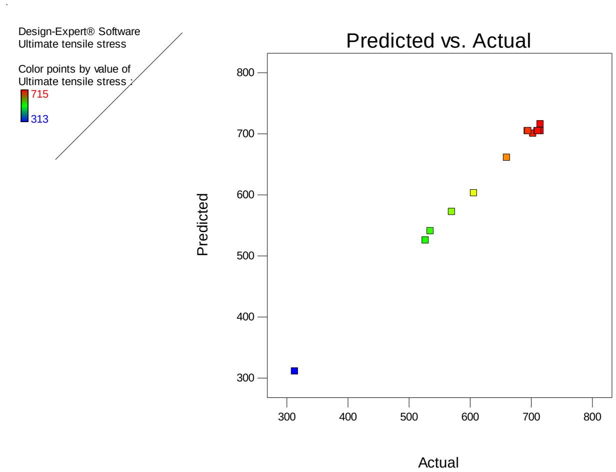

Figure (15): Predicted versus actual data

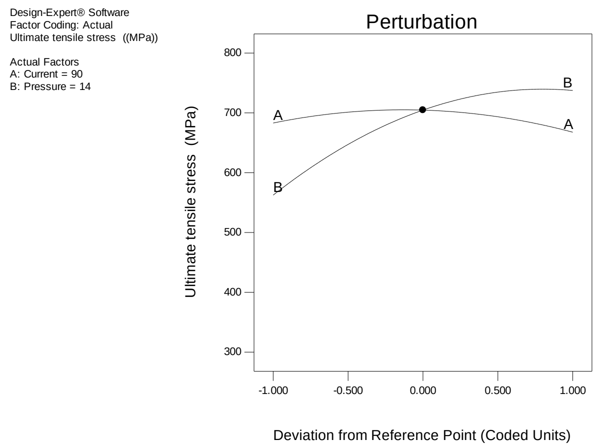

Figure (16): Perturbation of ultimate tensile stress

According to Figure 17 for the 2D contour graph, it can be noted that generally the ultimate tensile stress has the highest value at a higher level of gas pressure and almost at the center level of current (90 Amp). This means that the gas pressure has a greater impact on the ultimate tensile stress than current. This is ascribed to the significant protection of gas than the heat input caused by the current. It can also be seen that at the higher current and lower gas pressure, the ultimate tensile stress decreased due to the higher thermal effect resulted by the higher heat input. Where, Figure 18 reveals the 3D graph of ultimate tensile strength as a function of gas pressure and current and confirms that the increase of gas pressure increases the ultimate tensile stress at lower and higher level of current, while the increase of current is less influential at lower and higher level of gas pressure.

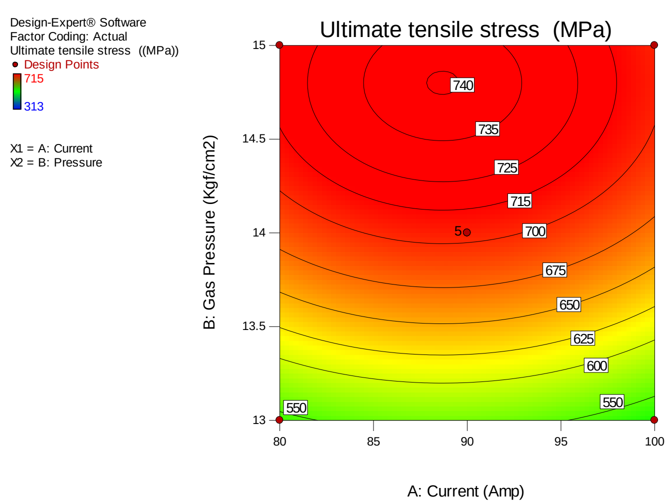

Figure (17): 2D contour graph of ultimate tensile stress as a function of current and gas pressure

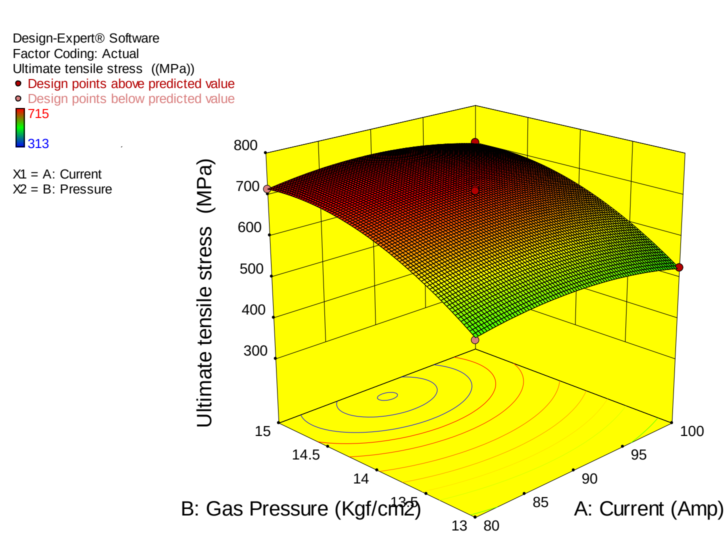

Figure (18): 3D surface plot of ultimate tensile stress as a function of current and gas pressure

4.3 The elongation model

The average responses obtained for the elongation percentage were used in calculating the models of the response surface per response using the least squares method. For elongation prediction, a reduced quadratic model in coded terms was analyzed with backwards elimination of insignificant coefficients. This models reveals that the terms (A), (B) and the interaction (AB) are significant with exception of the term (B2). This means that these three terms (current, gas pressure and the interaction of both factors) have the highest impact on elongation. Table 7 manifests the statistical analysis of variance (ANOVA) produced by the software for the remaining terms. The model is significant at 95% confidence. The lack of fit test indicates a good model.

Table 7: ANOVA for response surface quadratic model for elongation

Source	Sum of Squares	df	Mean Square	F Value	P-value Prob> F
Model	540.09	4	135.02	66.59	<0.0001**significant**
A-Current	75.00	1	75.00	36.99	0.0003
B-Gas Pressure	56.33	1	56.33	27.78	0.0008
AB	400.00	1	400.00	197.26	<0.0001
B^2	8.75	1	8.75	4.32	< 0.0714
Residual	16.22	8	2.03		
Lack of Fit	3.02	4	0.76	0.23	0.9088 **not significant**
Pure Error	13.20	4	3.30		
Cor Total	556.31	12			

Std. Dev.1.42	**R-Squared** 0.9708
Mean 33.77	**Adj. R-Squared** 0.9563
C.V. %4.22	**Pred. R-Squared**0.9489
PRESS28.43	**Adeq. Precision**23.308

The final equation of elongation in terms of the actual factors is:

Elongation = -1057.79630 + 13.75000 * Current +71.24074 * Gas Pressure

- 1.00000 * Current *Gas Pressure +0.59259 * Gas Pressure^2 ….**(3)**

For checking statistically the adequacy of the model, the normal probability plot for the elongation data shows that the residuals generally fall on a straight line, revealing that the errors, are normally distributed. Also, from the residuals versus predicted responses plot for the elongation data, it is noted that there are no clear patterns or unusual structure, depicting that the models are accurate.

Figure 19 displays the predicted actual elongation data versus the actual ones for comparison reason. Figure 20 shows the perturbation of ultimate tensile stress which views the effect of both current and gas pressure on the elongation over the range of the used levels; both gas pressure and current have a greater impact on the elongation. While, figure 21 exhibits that the interaction (combined influence) of both factors takes place after the center (about88 Amp current).

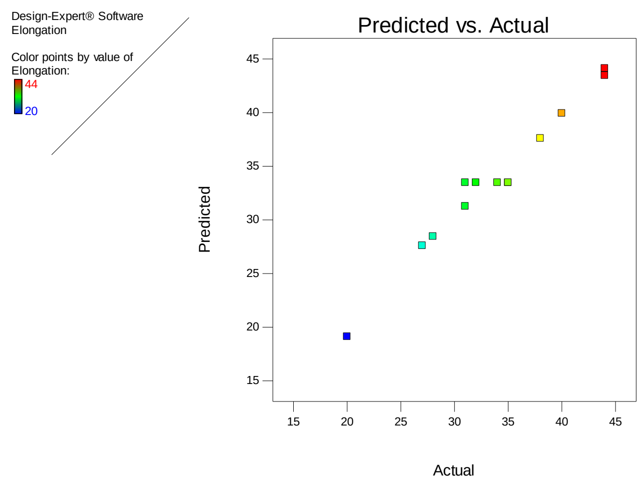

Figure (19): Predicted versus actual data

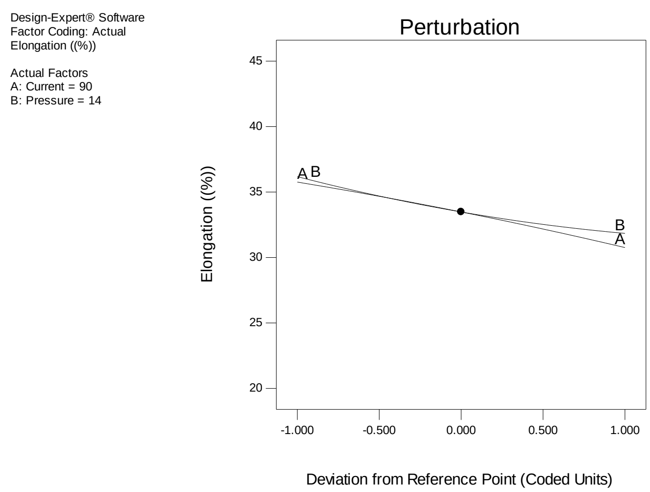

Figure (20): Perturbation of ultimate tensile stress

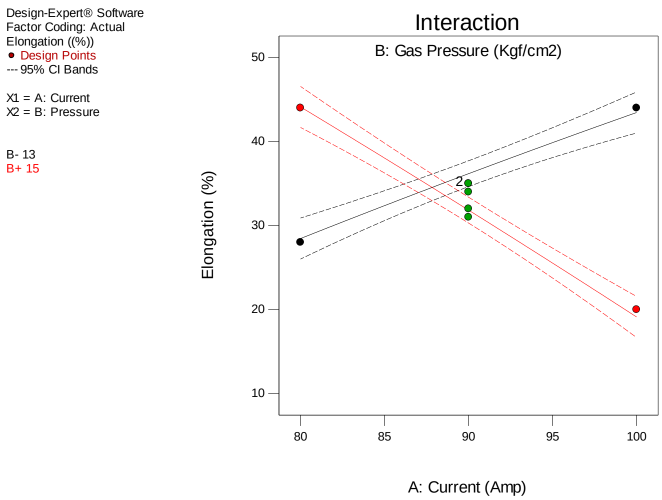

Figure (21): Interaction of the current with the gas pressure

Figure 22 demonstrates the 2D contour graph of elongation as a function of current and gas pressure.Referring to this figure, it can benoticed that the increase in both gas pressure and currentindividually leads to a higher increase in the elongation. The increase in the gas pressure at lower current (80 Amp)resulted inmore than (40%) elongation due to the more protection of the weld joint caused by the higher gas pressure,and the increase in the current (100 Amp) at lower gas pressure (13 Kgf/cm2) also resulted in more than (40%) elongation due to the higher thermal effect caused by the higher heat input at higher current. This means that both gas pressure and current have a greater influence on the elongation individually and they proportionate inversely. Regarding the interaction of gas pressure and current, this figure also shows that at almost (88 Amp and 14 Kgf/cm2), the combined influence of both factors gives a lower elongation(about 34%) elongation than that caused by each one individually.

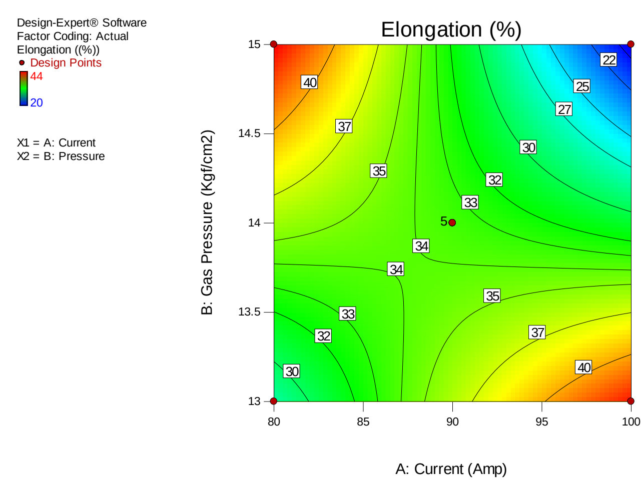

Figure (22): 2D contour graph of elongation as a function of current and gas pressure

Figure 23 clarifies the 3D graph (surface plot) of elongation as a function of gas pressure and current and confirms the observations mentioned in the 2D graph. It can be noted that the increase of both gas pressure and current resulted in an increase in the elongation value at their higher level, whereas at almost near their center level (design center point), they gave the lowest value of elongation.

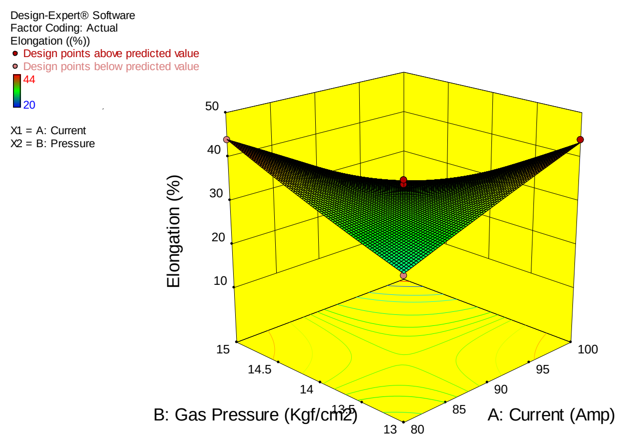

Figure (23): 3D surface plot of elongation as a function of current and gas pressure

4.4 Optimization of the mechanical properties

Numerical optimization was employed by the DOE software to obtain the optimum combinations of parameters in order to fulfill the desired requirements, depending on the results from the predictedquadratic models for the mechanical properties as responses (0.2% yield stress, ultimate tensile strength and elongation) as a function of two input factors (gas pressure and current).

To modify these predicted models, a new objective function called 'Desirability', which is an objective function, was evaluated and to be maximized through a numerical optimization, which ranges from 0 to 1 at the goal. The ultimate aim of this optimization was to find the maximum response that simultaneously met all the variable properties.Constrains of each variable for numerical optimization of the 0.2% yield stress, ultimate tensile strength and elongation were used, the input factors were selected for their used ranges, while the responses were selectedto be the maximum. Accordingly, one possible solutionsatisfied these constrains to find the maximum values of the mechanical properties (322.346 MPa yield stress, 715.943 MPa ultimate tensile stress and 44.148 % elongation), as shown in Table 8 with a maximum desirability value of (0.991) at the optimum values of gas pressure (15 Kgf/cm^2) and current (80Amp).

Table 8: The optimum values of input factors and outputs

Current (Amp)	Gas pressure (Kgf/cm^2)	0.2% Yield stress (MPa)	Ultimate tensile stress (MPa)	Elongation (%)	Desirability
80	15	322.346	715.943	44.148	0.991

4.5 Confirmation Tests at the Optimum Conditions

Confirmation tests were carried out at the optimum values of gas pressure and current to verify the validation of the maximum values of the mechanical properties shown in Table 8. The results of these confirmation tests are given Table 9 for the comparison purpose between the experimental and predicted results. According to the results listed in this table, the maximum error between the predicted and experimental error for 0.2% yield stress, ultimate tensile stress and elongation is less than (4%), (1%) and (1%), respectively.

Table 8: Results of confirmation tests at the optimum conditions

Current (Amp.)	Gas Pressure (Kgf/cm^2)	Exp. 0.2% Yield Stress (MPa)	Pred. Yield Stress (MPa)	Exp. Ultimate Tensile Stress (MPa)	Pred. Ultimate Tensile Stress (MPa)	Exp. Elongation (%)	Pred. Elongation (%)
80	15	335	322.346	715	715.943	44	44.148

5. Conclusions

1-The increase in both gas pressure and currentindividually leads to a higher increase in the 0.2% yield stress,and both input factors proportionate inversely. Their combined effect almost near their center level gives the lowest value of yield stress.

2-The gas pressure has a greater impact on the ultimate tensile stress than current. The increase of gas pressure increases the ultimate tensile stress at lower and higher level of current, while the increase of current is less influential at lower and higher level of gas pressure.

3-The increase in both gas pressure and currentindividually results in a higher increase in the elongation,and both input factors proportionate inversely. Their combined effect almost near their center level gives the lowest value of elongation.

4-Accordingly to the numerical optimization, the maximum values of the mechanical properties are (322.346 MPa yield stress, 715.943 MPa ultimate tensile stress and 44.148 % elongation) with a maximum desirability value of (0.991) at the optimum values of gas pressure (15 Kgf/cm^2) and current (80 Amp).

5- Confirmation tests manifested that the maximum errors between the predicted and experimental error for 0.2% yield stress, ultimate tensile stress and elongation are less than (4%), (1%) and (1%), respectively.

Conflicts of Interest

The author declares that they have no conflicts of interest.

References

[1] Arvinder Singh, Vanraj Kant Suman and Suri N.M, "Parameter optimization for tensile strength of spot weld for 316L stainless steel", *International Journal of Scientific & Engineering Research*,Vol. 4, Issue 7, 2013, pp.2443-2446.

[2] Larry F. Jeffus,"Welding and Metal Fabrication”,*Publisher Cengage Learning*, 1st Edition, 2012.

[3] Lakshman Singh, Vinay Shah and Naveen K.Singh,"The Influence of TIG Welding Parameters on Weld Characteristics of 5083 Aluminum Alloy",*International Journal of Engineering Science and Innovative Technology*, Vol.2, Issue5, 2013.

[4] Naitik S. Patel, and Rahul B. Patel, "A Review on Parametric Optimization of Tig Welding",*International Journal of Computational Engineering Research*, Vol. 4, Issue 1, 2014.

[5] Radha Raman Mishra1, Visnu Kumar Tiwari, and Rajesha S.,"A StudyofTensileStrengthof MIG and TIG WeldedDissimilarJointsofMildSteelandStainlessSteel",*International Journal of Advances in Materials Science and Engineering (IJAMSE)*,Vol.3, No.2,April 2014.

[6] V.Anand Raoam and R.Deivanathanb,"Experimental Investigation for Welding Aspects of Stainless Steel 310 for the Process of TIG Welding", *12th GlobalCongress OnManufacturingandManagement, GCMM*, 2014.

[7] C. Prabaharan, P. Venkatachalam, K. Suresh kumar and K. Lenin, "Parametric Optimization of Gas Tungsten Arc Welding Processes by Using Factorial Design Approach", *Journal of Scientific & Industrial Research*,Vol.73, pp. 415-420,June 2014.

[8] Ravinder, S. K. Jarial,"Parametric Optimization of TIG Welding on Stainless Steel (202) & Mild Steel by using Taguchi Method",*International Journal of Enhanced Research in Science Technology & Engineering*, Vol.4, Issue 6, pp.484-494,June 2015.

[9] Gurdev Singh and Aman Bansal,"ParametricOptimizationof TIG WeldingonStainlessSteel",*An International Journal of Engineering Sciences*, Vol. 21, Issue December, 2016.

[10] M.Ravichandran, A. Naveen Sait, and U. Vignesh," Investigation on TIG welding parameters of 2205 duplex stainless steel", *International Journal of Automotive and Mechanical Engineering*, Vol. 14, Issue 3, pp. 4518-4530, September 2017.

[11] Kumar Rahul Anand, and Vijay Mittal, " ParametricOptimizationof TIG WeldingonJointofStainlessSteel(316) &MildSteelUsingTaguchi Technique", *International Research Journal of Engineering and Technology*,Vol.4, Issue 5, May 2017.

[12] ASTM, "Standard Specification for Heat-Resisting Chromium and Chromium-Nickel Stainless Steel Plate, Sheet, and Strip for Pressure Vessels", *A240*, 2006.

[13]ASTM, "Standard Test Methods for Tension Testing of Metallic Materials", *E8/E8M – 09*, 2006.

دراسة تأثير ضغط جريان الغاز على سلوك الشد لصفائح الفولاذ المقاوم للصدأ الملحومة بالتيج

سمير علي أمين   لمياء مهدي أسعد   علي حسين علوان

قسم الهندسة الميكانيكية، الجامعة التكنولوجية، بغداد، العراق

eng.ali83@yahoo.com   lmy_asr@yahoo.com   alrabiee2002@yahoo.com

الخلاصة:

يمثل عمل هذا البحث دراسة تأثير استخدام ضغوط مختلفة لغاز الاركون على سلوك الشد لصفائح الفولاذ المقاوم للصدأ نوع (٣٠٤) الملحومة بغاز التنجستن الخامل. استخدمت مديات مختلفة من ضغوط الغاز (١٥-١٣)كغم قوة/سم^٢ وتيارات لحام (١٠٠-٨٠) أمبيرلأيجاد تاثيراتها على خواص الشد الميكانيكية (٠,٢% اجهاد الخضوع، اجهاد الشد الاقصى والاستطالة) لوصلاتاللحام التناكبية.تم استخدام برنامج تصميم التجارب(DOE) (نسخة ١٠) لعمل مصفوفة التجارب. تم تطبيق منهجية الاستجابة السطحية (RSM) لأيجاد النماذج الرقمية للخواص الثلاثة والتي تم تحليلها بأستخدام تحليل التباين (ANOVA) للتحقق احصائيا" من ملائمة النماذج الناتجة. اظهرت النماذج التربيعية المستحصلة بمستوى ثقة (٩٥%) بأن الزيادة في كل من ضغط الغاز والتيار بشكل منفصل ادت الى زيادة عالية في اجهاد الخضوع والاستطالة وكلاهما تناسب عكسيا"، بينما اعطى التأثير المشترك لهما القيم الادنى. كان لضغط الغاز تأثيرا كبيرا" على اجهاد الشد الاقصى من التيار.

الكلمات الداله:- لحام التيج، ضغط الغاز، الخواص الميكانيكية، تصميم التجارب، منهجية الاستجابة السطحية، الامثلية العددية.